

A No-Scale Inflationary Model to Fit Them All

John Ellis^a, Marcos A. G. García^b, Dimitri V. Nanopoulos^c
and
Keith A. Olive^b

^a*Theoretical Particle Physics and Cosmology Group, Department of Physics,
King's College London, London WC2R 2LS, United Kingdom;
Theory Division, CERN, CH-1211 Geneva 23, Switzerland*

^b*William I. Fine Theoretical Physics Institute, School of Physics and Astronomy,
University of Minnesota, Minneapolis, MN 55455, USA*

^c*George P. and Cynthia W. Mitchell Institute for Fundamental Physics and Astronomy,
Texas A&M University, College Station, TX 77843, USA;
Astroparticle Physics Group, Houston Advanced Research Center (HARC), Mitchell
Campus, Woodlands, TX 77381, USA;
Academy of Athens, Division of Natural Sciences, Athens 10679, Greece*

ABSTRACT

The magnitude of B-mode polarization in the cosmic microwave background as measured by BICEP2 favours models of chaotic inflation with a quadratic $m^2\phi^2/2$ potential, whereas data from the Planck satellite favour a small value of the tensor-to-scalar perturbation ratio r that is highly consistent with the Starobinsky $R + R^2$ model. Reality may lie somewhere between these two scenarios. In this paper we propose a minimal two-field no-scale supergravity model that interpolates between quadratic and Starobinsky-like inflation as limiting cases, while retaining the successful prediction $n_s \simeq 0.96$ and predicting very little non-Gaussianity: $f_{NL}^{(4)} \lesssim 0.1$.

April 2014

1 Introduction

The theory of inflationary cosmology has received important boosts from the first release of data from the Planck satellite [1] - which confirmed the infrared tilt of the scalar perturbation spectrum n_s [2] expected in slow-roll models of inflation [3] - and the discovery by BICEP2 of B-mode polarization fluctuations [4] - which may be interpreted as primordial tensor perturbations with a large ratio r relative to the scalar perturbations, as would be generated in models with a large energy density during inflation. On the other hand, whereas Planck and BICEP2 agree with earlier WMAP data that $n_s \simeq 0.96$, there is tension between the BICEP2 measurement $r = 0.16_{-0.05}^{+0.06}$ (after dust subtraction) and the Planck upper limit on r obtained indirectly from the temperature fluctuations at low multipoles [5]. Theoretically, this tension could be reduced by postulating large running of the scalar spectral index, but this would require a large deviation from the hitherto successful slow-roll inflationary paradigm. Experimentally, it is known that the temperature perturbations in the Planck data [1] lie somewhat below the standard inflationary predictions at low multipoles, and there is a hint of a hemispherical asymmetry, so perhaps the inflationary paradigm does indeed require some modification [6]. On the other hand, verification of the dust model used by BICEP2 is desirable, and other possible sources of foreground contamination such as magnetized dust associated with radio loops need to be quantified [7]. The good news is that the experimental situation should be clarified soon, with additional data from Planck, the Keck Array and other B-mode experiments.

In the mean time, inflationary theorists are having a field day exploring models capable of accommodating the BICEP2 and/or Planck data. Taken at face value, the BICEP2 data are highly consistent with the simplest possible chaotic $m^2\phi^2/2$ potential [8] that predicts $r \simeq 0.16$, whereas the Planck data tend to favour the Starobinsky $R+R^2$ model [9–11] that predicts $r \simeq 0.003$. It seems very likely that experimental measurements of r may settle down somewhere between these limiting cases, so it is interesting to identify models that interpolate between them, while retaining the successful prediction $n_s \simeq 0.96$. Desirable features of such models would include characteristic predictions for other inflationary observables and making connections with particle physics.

With the latter points in mind, we consider the natural framework for formulating models of inflation to be supersymmetry [12–16], specifically local supersymmetry, i.e., supergravity [17]. Moreover, in order to avoid holes in the effective potential with depths that are $\mathcal{O}(1)$ in Planck units and to address the η problem [18], we favour no-scale supergravity [19, 20], which has the theoretical advantage that it emerges naturally as the low-energy effective field theory derived from compactified string theory [21]. In the past we [22–26] and others [27–33] have shown how no-scale supergravity with a Wess-Zumino or other superpotential [34] leads naturally to Starobinsky-like inflation, and more recently

we [26] and others [35–43] have given examples how quadratic inflation may be embedded in no-scale supergravity.

In this paper we introduce a minimal two-field no-scale supergravity model with a Kähler potential motivated by orbifold compactifications of string theory [44, 45]. Unlike previous attempts at inflationary models in this context, the model presented below requires no additional terms in either the Kähler potential or superpotential to stabilize field directions coupled to inflation*. The initial condition for the inflaton field has a free parameter that which can be regarded as an angle in the two-field space. Varying this angle, we can interpolate between the quadratic and Starobinsky-like limits: $0.16 \gtrsim r \gtrsim 0.003$ †, while $n_s \simeq 0.96$ varies very little with the interpolating parameter. We follow numerically the evolution of the inflaton in this space, including the possibility of initial values of the inflaton fields that are larger than the minimal values need to obtain sufficient e-folds, and verify that the model predicts a very low level of non-Gaussianity [46]: $f_{NL}^{(4)} \lesssim 0.1$ ‡. The key model predictions are insensitive to the mechanism of supersymmetry breaking, as long as it occurs at some scale much less than the inflaton mass. We illustrate this via a Polonyi example of supersymmetry breaking, and comment on the connection to particle phenomenology in this model.

The structure of this paper is as follows. In Section 2 we specify our model, and in Section 3 we provide numerical analyses of inflationary scenarios with different initial conditions for the inflaton field, discussing its predictions for n_s, r and $f_{NL}^{(4)}$. Then, in Section 4 we discuss briefly supersymmetry breaking, and in Section 5 we draw some conclusions.

2 Specification of the Model

The original, minimal no-scale supergravity model has a Kähler potential of the form [19]

$$K = -3 \ln(T + \bar{T}) + \dots, \quad (1)$$

where the dots represent a possible superpotential, terms involving additional matter fields, etc.. Subsequent to its discovery, it was shown that no-scale supergravity emerges naturally as the low-energy effective field theory in generic string compactifications [21]. In general,

*Though we do include strong stabilization when we include supersymmetry breaking contributions.

†One might have thought that [32] would provide a suitable framework for achieving this. However, the Starobinsky-like limit is lost when the Kähler potential is stabilized as discussed in [26, 33].

‡Small levels of non-Gaussianity were also found recently [47] in a globally-supersymmetric two-field model [48] that can yield smaller r than quadratic inflation.

these contain the complex moduli $T_i : i = 1, 2, 3$, and (1) becomes

$$K = -\sum_{i=1}^3 \ln(T_i + \bar{T}^i) + \dots \quad (2)$$

In the specific case of orbifold compactifications of string, matter fields ϕ have non-zero modular weights and appear in a Kähler potential term of the form [44]

$$\Delta K = \frac{|\phi|^2}{\prod_{i=1}^3 (T_i + \bar{T}^i)}. \quad (3)$$

For simplicity, we consider here the case where the ratios of the three orbifold moduli are fixed at a high scale by some unspecified mechanism so that, neglecting irrelevant constants, the Kähler potential may be written in the form [45]:

$$K = -3 \ln(T + \bar{T}) + \frac{|\phi|^2}{(T + \bar{T})^3}. \quad (4)$$

Thus we assume that the field ϕ has modular weight -3 , and stress that the special properties of the model we describe below depend on this choice of modular weight. More general constructions of Minkowski and deSitter vacua were discussed in a similar context in [49], which focused on models where the modular weight of ϕ is 0.

The specification of our no-scale supergravity model of inflation is completed by specifying the superpotential:

$$W = \sqrt{\frac{3}{4}} \frac{m}{a} \phi (T - a), \quad (5)$$

and we identify T as the chiral (two-component) inflaton superfield. Although the superpotential (5) is the same as in the model [34] derived in a realization of $R + R^2$ gravity in a $SU(2,1)/SU(2) \times U(1)$ no-scale model, the Kähler potential (4) manifests only the minimal $SU(1,1)/U(1)$ no-scale structure. The scalar potential is derived from the Kähler potential (4) and the superpotential (5) through

$$V = e^K \left(K^{i\bar{j}} D_i W \bar{D}_{\bar{j}} \bar{W} - 3|W|^2 \right), \quad (6)$$

where $D_i W \equiv \partial_i W + K_i W$. We will work in Planck units $M_P^2 = 8\pi G_N = 1$. The motion of the scalar field ϕ is constrained by the exponential factor e^K :

$$V \propto e^{|\phi|^2/(T+\bar{T})^3} \simeq e^{(2a)^{-3}|\phi|^2}. \quad (7)$$

For $a \leq 1$, it can be assumed (and we have verified) that ϕ is rapidly driven to zero at the onset of inflation, and we assume that $a = 1/2$ so that ϕ has a canonical kinetic term. For vanishing ϕ , the scalar potential takes the simple form

$$V = \frac{3m^2}{4a^2} |T - a|^2 \quad (8)$$

which can be shown to be equivalent to the Starobinsky model along the real direction of the canonical field associated with T [23, 27, 34]. For other choices of the modular weight w of ϕ , the potential (at $\phi = 0$) is

$$V = \frac{3m^2}{4a^2} |T - a|^2 (T + T^*)^{-(w+3)}. \quad (9)$$

It is convenient to decompose T into its real and imaginary parts defined by ρ and σ , respectively, where ρ is canonical and σ is canonical at the minimum when $\rho = 0$:

$$T = a \left(e^{-\sqrt{\frac{2}{3}}\rho} + i\sqrt{\frac{2}{3}}\sigma \right) \quad (10)$$

The scalar component of T minimizes the potential when $T = a$, and the resulting Lagrangian is given by

$$\begin{aligned} \mathcal{L} = & \frac{1}{2} \partial_\mu \rho \partial^\mu \rho + \frac{1}{2} e^{2\sqrt{\frac{2}{3}}\rho} \partial_\mu \sigma \partial^\mu \sigma \\ & - \frac{3}{2^{(w+5)} a^{(w+3)}} m^2 e^{\sqrt{\frac{2}{3}}(w+3)\rho} \left(1 - e^{-\sqrt{\frac{2}{3}}\rho} \right)^2 \\ & - \frac{1}{2^{(w+4)} a^{(w+3)}} m^2 e^{\sqrt{\frac{2}{3}}(w+3)\rho} \sigma^2. \end{aligned} \quad (11)$$

In the particular case $w = -3$ this reduces to

$$\mathcal{L} = \frac{1}{2} \partial_\mu \rho \partial^\mu \rho + \frac{1}{2} e^{2\sqrt{\frac{2}{3}}\rho} \partial_\mu \sigma \partial^\mu \sigma - \frac{3}{4} m^2 \left(1 - e^{-\sqrt{\frac{2}{3}}\rho} \right)^2 - \frac{1}{2} m^2 \sigma^2, \quad (12)$$

which is the starting-point for our analysis.

Although this is similar to the Lagrangian for the no-scale model of [32, 34], it differs in an important way. In that $\text{SU}(2,1)/\text{SU}(2) \times \text{U}(1)$ model, the mass term for σ contained a coupling to ρ of the form $e^{2\sqrt{2/3}\rho}$. As a result, quadratic chaotic inflation is not possible, as the field tends to evolve towards large ρ with subsequent evolution similar to the Starobinsky model [26, 32, 33]. Quadratic chaotic inflation can be recovered only when stabilization terms of the form $(T+T^*)^2$ and $(\phi\phi^*)^2$ terms are added to the Kähler potential. In (12) no such stabilization terms are necessary, as the real and imaginary parts of T are decoupled in the potential and only mix through their kinetic terms (we return later to the effect of this mixing).

The minimum of the effective potential (12) in the (ρ, σ) plane is located at

$$\rho_0 = \sigma_0 = 0. \quad (13)$$

When ρ is at the minimum, the effective Lagrangian for σ is

$$\mathcal{L} = \frac{1}{2} \partial_\mu \sigma \partial^\mu \sigma - \frac{1}{2} m^2 \sigma^2, \quad (14)$$

and we recover the minimal quadratic inflationary model. Conversely, when σ is at the minimum, the effective Lagrangian for ρ is

$$\mathcal{L} = \frac{1}{2}\partial_\mu\rho\partial^\mu\rho - \frac{3}{4}m^2\left(1 - e^{-\sqrt{\frac{2}{3}}\rho}\right)^2, \quad (15)$$

which is of the same form as the Starobinsky model [9].

Various slices through the potential (12) for the canonical choice $a = 1/2$ are shown in Fig. 1. In the upper left panel we see the characteristic Starobinsky form in the ρ direction (15) and the simple quadratic form in the σ direction (14). In the upper right panel we see that both the real and imaginary parts of ϕ are indeed stabilized at zero, the value that was assumed in the upper left panel. The lower left panel shows that the effective potential is well-behaved in the $(\sigma, \text{Re } \phi)$ plane for $\rho = \text{Im } \phi = 0$, and the lower right panel makes the same point for the $(\rho, \text{Re } \phi)$ plane for $\sigma = \text{Im } \phi = 0$. In both cases, the effective potential is identical when the rôles of $\text{Re } \phi$ and $\text{Im } \phi$ are reversed. The Starobinsky form of potential is visible again in the lower right panel of Fig. 1.

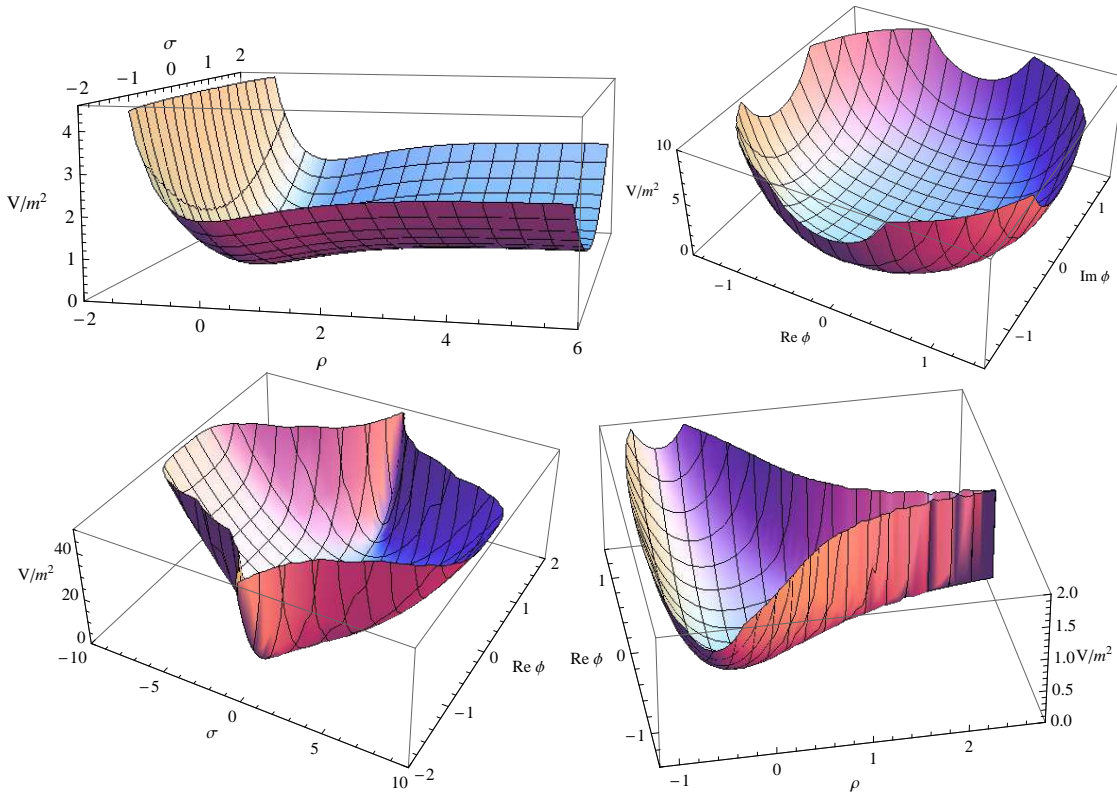


Figure 1: *Slices through the effective potential for the model (12). Upper left: The potential in the (ρ, σ) plane for $\phi = 0$. Upper right: The potential in the $(\text{Re } \phi, \text{Im } \phi)$ plane for $\rho = \sigma = 0$. Lower left: The potential in the $(\sigma, \text{Re } \phi)$ plane for $\rho = \text{Im } \phi = 0$. Lower right: The potential in the $(\rho, \text{Re } \phi)$ plane for $\sigma = \text{Im } \phi = 0$.*

3 Numerical Analysis of the Model

We have calculated numerically the motion of the inflaton field, solving the equations

$$H^2 = \frac{1}{3} \left[K_{a\bar{b}} \dot{\Psi}^a \dot{\Psi}^{\bar{b}} + V(\Psi) \right] = (\dot{N})^2, \quad (16)$$

$$\ddot{\Psi}^a + 3H\dot{\Psi}^a + \Gamma_{bc}^a \dot{\Psi}^b \dot{\Psi}^c + K^{a\bar{b}} \frac{\partial V}{\partial \bar{\Psi}^b} = 0, \quad (17)$$

where $\Psi \equiv (T, \phi)$, $K_{a\bar{b}}$ is the Kähler metric, $\Gamma_{bc}^a \equiv K^{a\bar{d}} \partial_b K_{c\bar{d}}$, and N is the number of e-foldings. The figures that follow show the resulting evolution for the T and ϕ fields for four different choices of initial conditions. In each case, we calculate the corresponding values of the scalar tilt n_s and the tensor-to-scalar ratio r using the formulae

$$\epsilon = \frac{3}{2} (1 + w), \quad \eta = 2\epsilon - \frac{\dot{\epsilon}}{2\epsilon H}, \quad n_s = 1 - 6\epsilon + 2\eta, \quad r = 16\epsilon, \quad (18)$$

where w is the equation of state parameter (not to be confused with the modular weight discussed above). The choices of initial values are intended to be illustrative of the possibilities, but not necessarily exhaustive.

Figs. 2 and 3 display the numerical solution for the initial conditions $\rho_0 = 0$, $\sigma_0 = 18$, $\phi_0 = 0$, corresponding to the case of quadratic inflation. The top panel of Fig. 2 shows the evolution of σ , which is the inflaton field in this case. The second panel of Fig. 2 displays the evolution of ρ . We note a perturbation of ρ that is due to its coupling with σ through the kinetic term (see (12)). However, the value of ρ remains small and does not affect substantially the inflationary dynamics of the inflaton field. The third panel shows that $\text{Re}\phi$ remains zero (and the same is true for $\text{Im}\phi$). Finally, the bottom panel of Fig. 2 displays the growth of the number of e-folds for this choice of boundary conditions. We find the following values of n_s and r for this case:

$$\begin{aligned} N = 50 : \quad (n_s, r) &= (0.959, 0.190), \\ N = 60 : \quad (n_s, r) &= (0.966, 0.162). \end{aligned} \quad (19)$$

As already commented, small values of ρ are generated during the evolution of the inflaton field, and Fig. 3 displays the joint evolution of ρ and σ , where we see a ‘circling the drain’ phenomenon towards the end of inflation. This does not have a significant effect on either n_s or r , and we show later that it does not give rise to large values of the non-Gaussianity parameter $f_{NL}^{(4)}$.

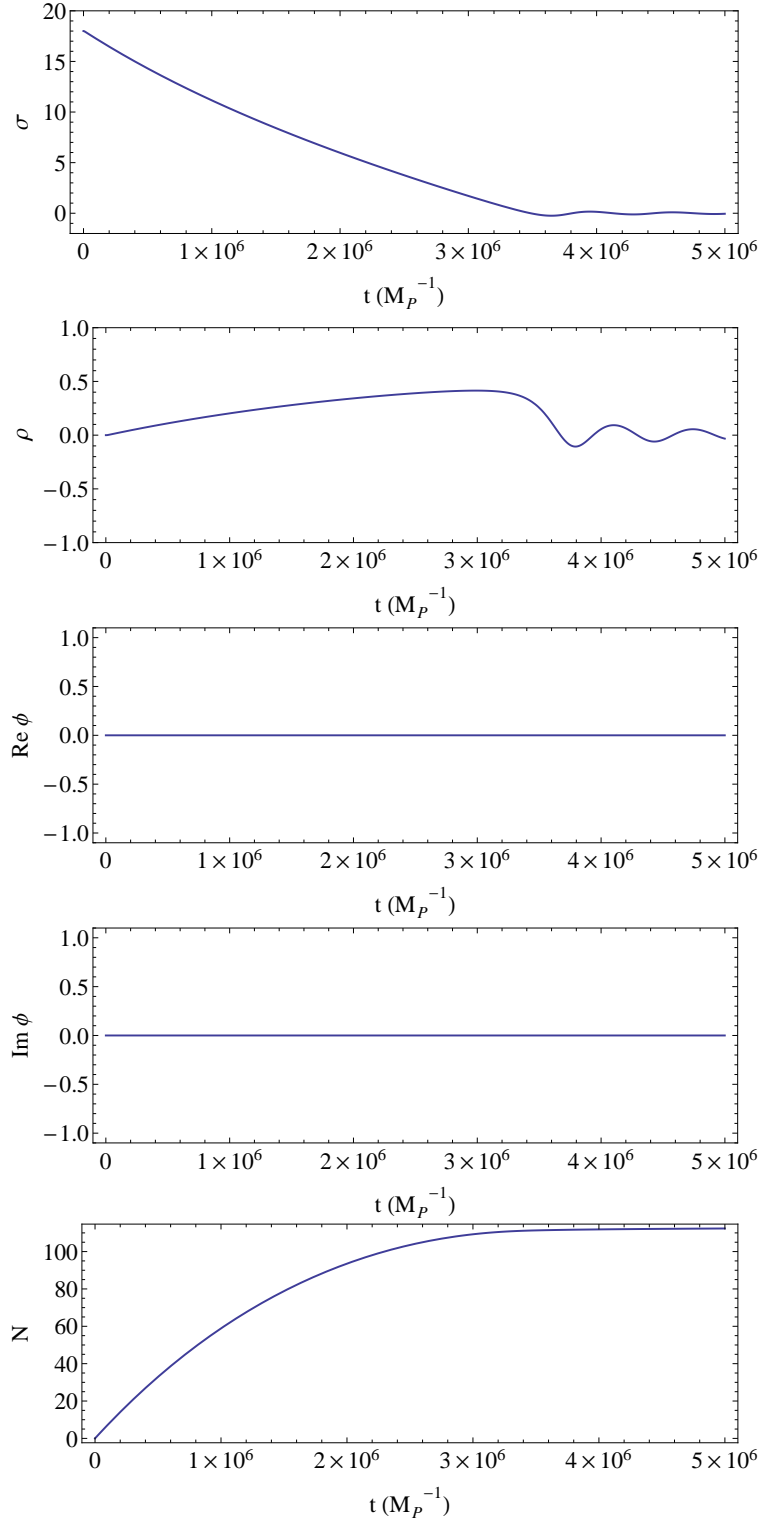


Figure 2: Numerical solution for the initial conditions $\rho_0 = 0$, $\sigma_0 = 18$, $\phi_0 = 0$: field evolution and e-folds.

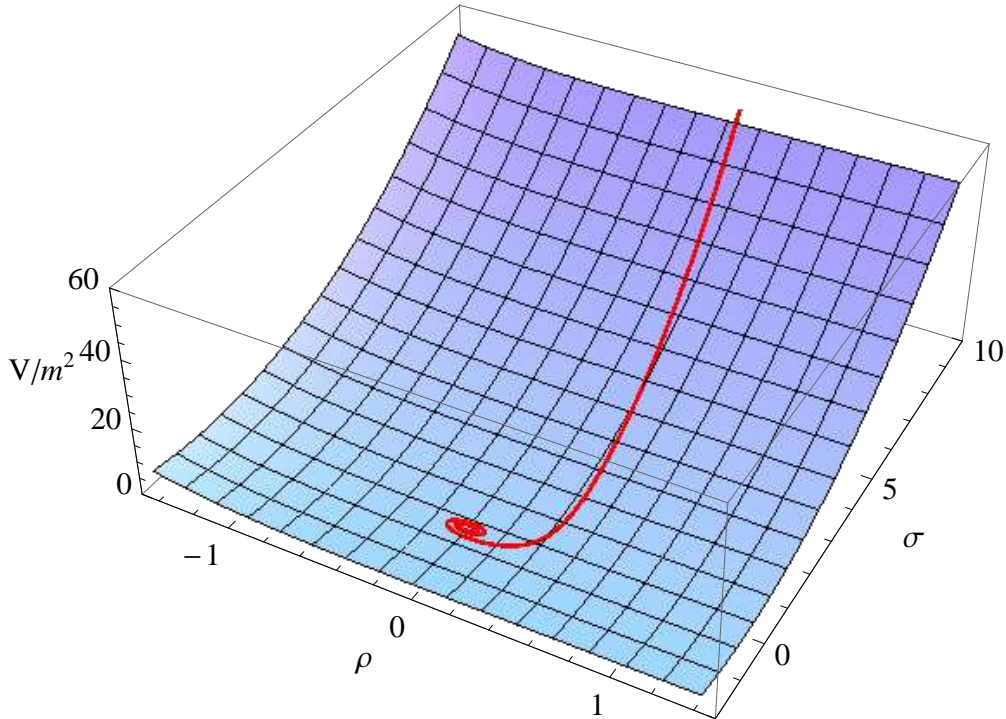


Figure 3: *Numerical solution for the initial conditions $\rho_0 = 0$, $\sigma_0 = 18$, $\phi_0 = 0$: ‘circling the drain’.*

Fig. 4 displays the numerical solution for the initial conditions $\rho_0 = 0$, $\sigma_0 = 18$, $\phi_0 = 0.4 + 0.4i$, corresponding to a modification of the previous case of quadratic inflation, allowing for non-trivial evolution of ϕ . However, we see in the top panels of Fig. 4 that both $\text{Re } \phi$ and $\text{Im } \phi$ evolve rapidly to zero, as expected, and ρ behaves similarly to the first case above (third panel). Correspondingly, the behaviour of the inflaton σ is also similar (fourth panel), and the number of e-folds grows in a similar way as in the first case. We find that

$$\begin{aligned}
 N = 50 : (n_s, r) &= (0.959, 0.188), \\
 N = 60 : (n_s, r) &= (0.966, 0.161),
 \end{aligned}
 \tag{20}$$

results that are very similar to the first case.

As a third example, displayed in Fig. 5, we show the evolution of the fields and the number of e-folds for Starobinsky-like initial conditions: $\rho_0 = 6.15$, $\sigma_0 = 0$, $\phi_0 = 0$. The top panel of Fig. 5 shows that, as expected, the inflaton field (ρ in this case) moves slowly initially, but then accelerates rapidly towards zero as it rolls down the steepening potential, before exhibiting damped oscillations. The second, third and fourth panels of Fig. 5 show that, also as expected, the other fields σ , $\text{Re } \phi$ and $\text{Im } \phi$ all remain fixed at their minima,

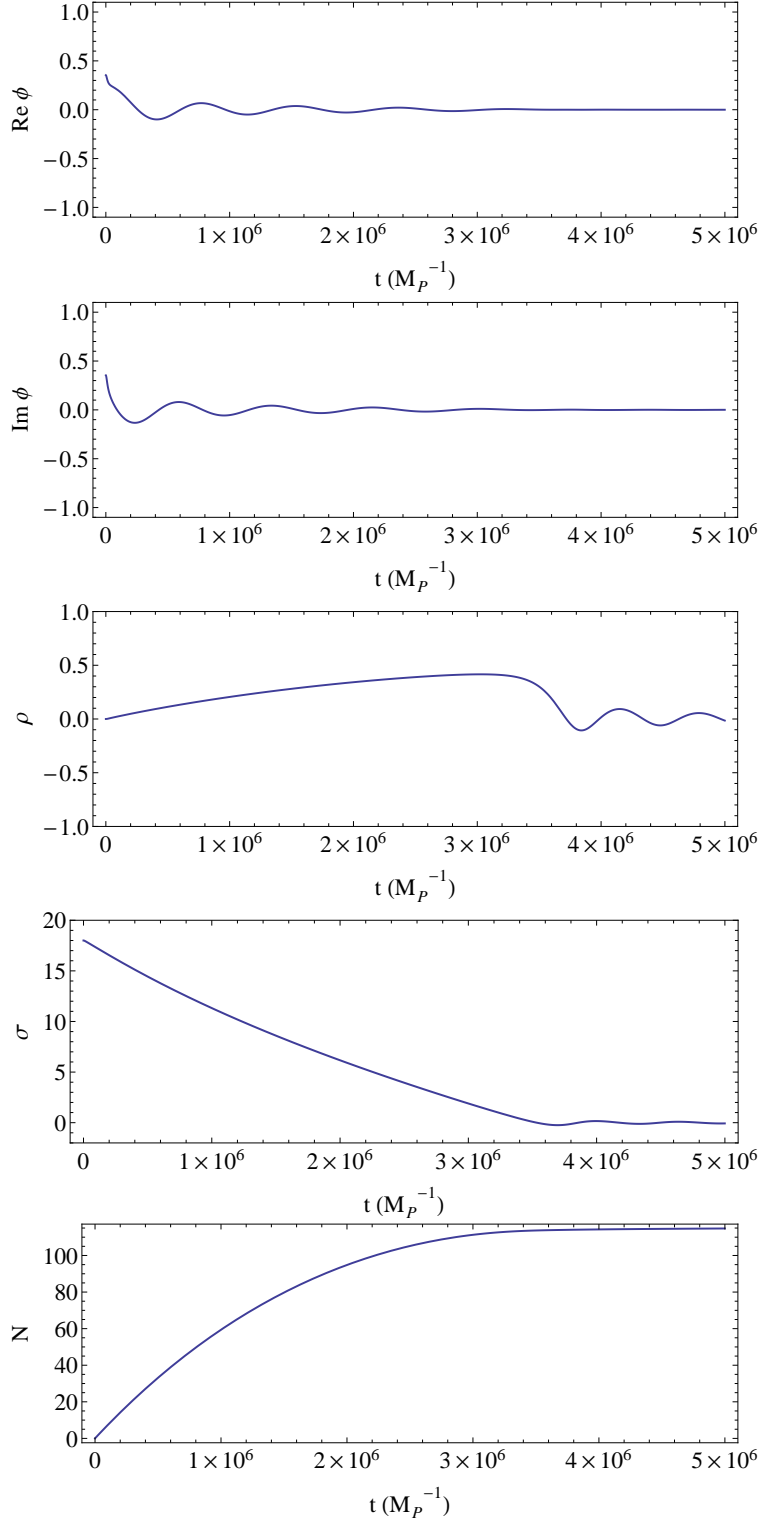


Figure 4: Numerical solution for the initial conditions $\rho_0 = 0$, $\sigma_0 = 18$, $\phi_0 = 0.4 + 0.4i$.

and the bottom panel displays the growth in the number of e-folds. We find for this set of initial conditions that

$$\begin{aligned} N = 50 : (n_s, r) &= (0.961, 0.0044), \\ N = 60 : (n_s, r) &= (0.967, 0.0031). \end{aligned} \tag{21}$$

Finally, Fig. 6 displays the results of including a small non-zero value of ϕ in the initial conditions: $\rho_0 = 6.15$, $\sigma_0 = 0$, $\phi_0 = 0.001 + 0.001i$. We choose $|\phi_0| \ll 1$ for $\rho > 1$ because, as seen in the lower right panel of Fig. 1, the effective potential rises very steeply as a function of ϕ when ρ is large. We see in the top two panels that ρ and σ evolve almost identically as before, whereas the third and fourth panels show that $\text{Re } \phi$ and $\text{Im } \phi$ exhibit small oscillations as inflation comes to an end. However, this has negligible effect of the growth in the number of e-folds, as seen in the bottom panel of Fig. 6. We find for this case that

$$\begin{aligned} N = 50 : (n_s, r) &= (0.961, 0.0044), \\ N = 60 : (n_s, r) &= (0.968, 0.0031), \end{aligned} \tag{22}$$

results that are very similar to the previous pure Starobinsky case.

It is clear from the above results that the scalar tilt and the tensor-to-scalar ratio depend on the initial condition for the complex inflaton field T . In order to quantify this dependence more generally, we consider general initial conditions in the (ρ, σ) plane parametrized by an angle θ , as shown in Fig. 7, restricting our attention to the case $\phi_0 = 0$. The resulting θ dependences of the inflationary observables n_s and r are displayed in Figs. 8 and 9. We see in the upper panel of Fig. 8 that n_s is almost independent of θ , and always within the 68% CL range favoured by WMAP [2], Planck [1] and BICEP2 [4]. On the other hand, we see in the lower panel of Fig. 8 that, as expected, r decreases monotonically from the large BICEP2-friendly values $r \gtrsim 0.16$ at $\theta = 0$ to the much smaller Planck-friendly values at $\theta = \pi/2$. We note that the results are symmetric under reflection in the ρ axis: $\theta \rightarrow \pi - \theta$, and that initial conditions $0 > \theta > -\pi/2$ (and their reflections) would give larger values of r than quadratic inflation or simply not inflate due to the exponential nature of the potential when $\rho < 0$. It is interesting to note that Fig. 8 exhibits an approximate ‘plateau’ for $\pi/8 < \theta < 3\pi/8$ where $r \sim 0.1$, which is compatible at around the 68% CL with both Planck and BICEP2. We complete this discussion of the θ dependence of r and θ by displaying in Fig. 9 the parametric curve $(n_s(\theta), r(\theta))$. Here we see clearly how the model (12) interpolates directly between the limits of quadratic and Starobinsky-like inflation.

So far, we have considered initial conditions for the fields with vanishing time derivatives: a ‘standing start’. One may, instead, consider stationary initial conditions with

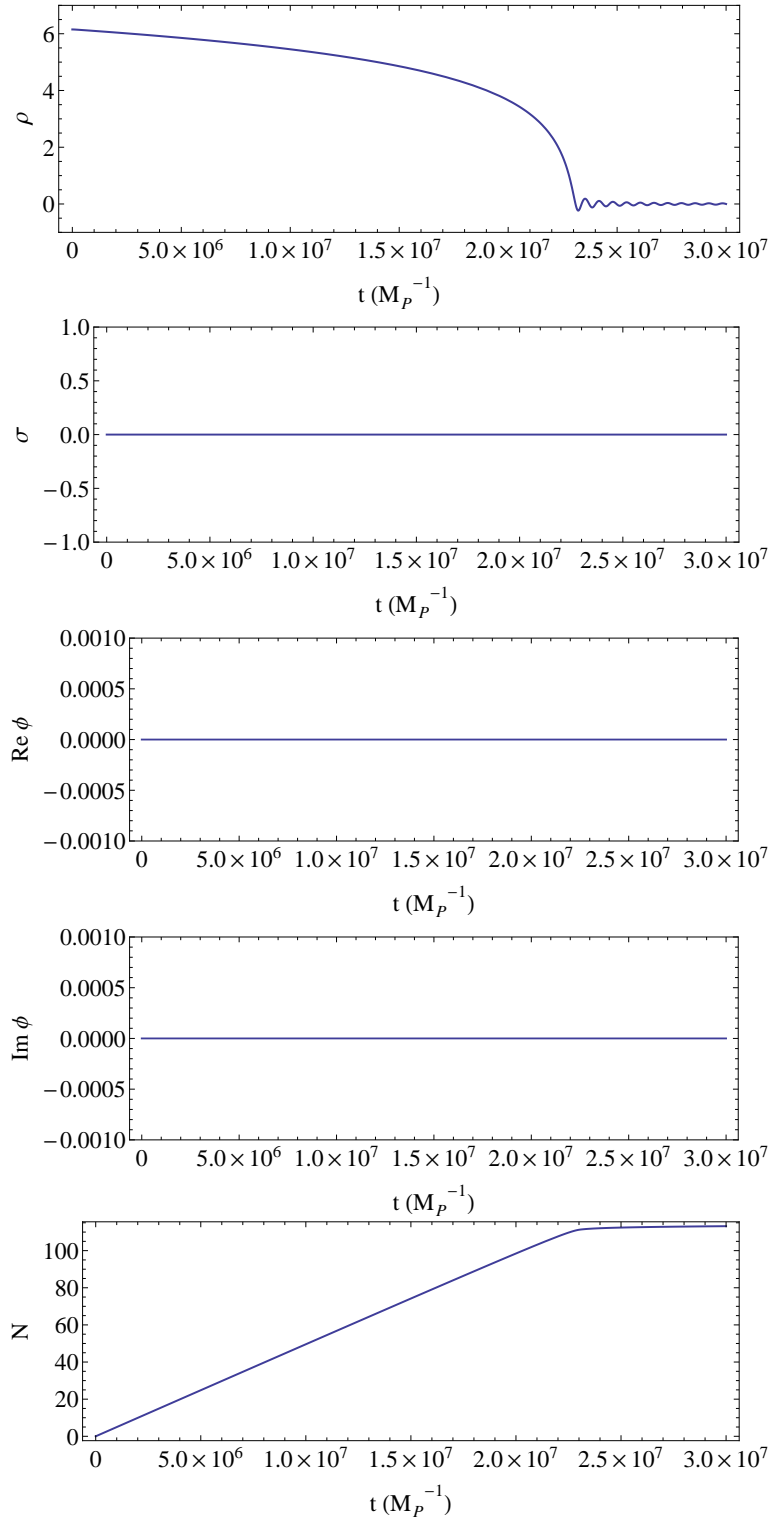


Figure 5: Numerical solution for the initial conditions $\rho_0 = 6.15$, $\sigma_0 = 0$, $\phi_0 = 0$.

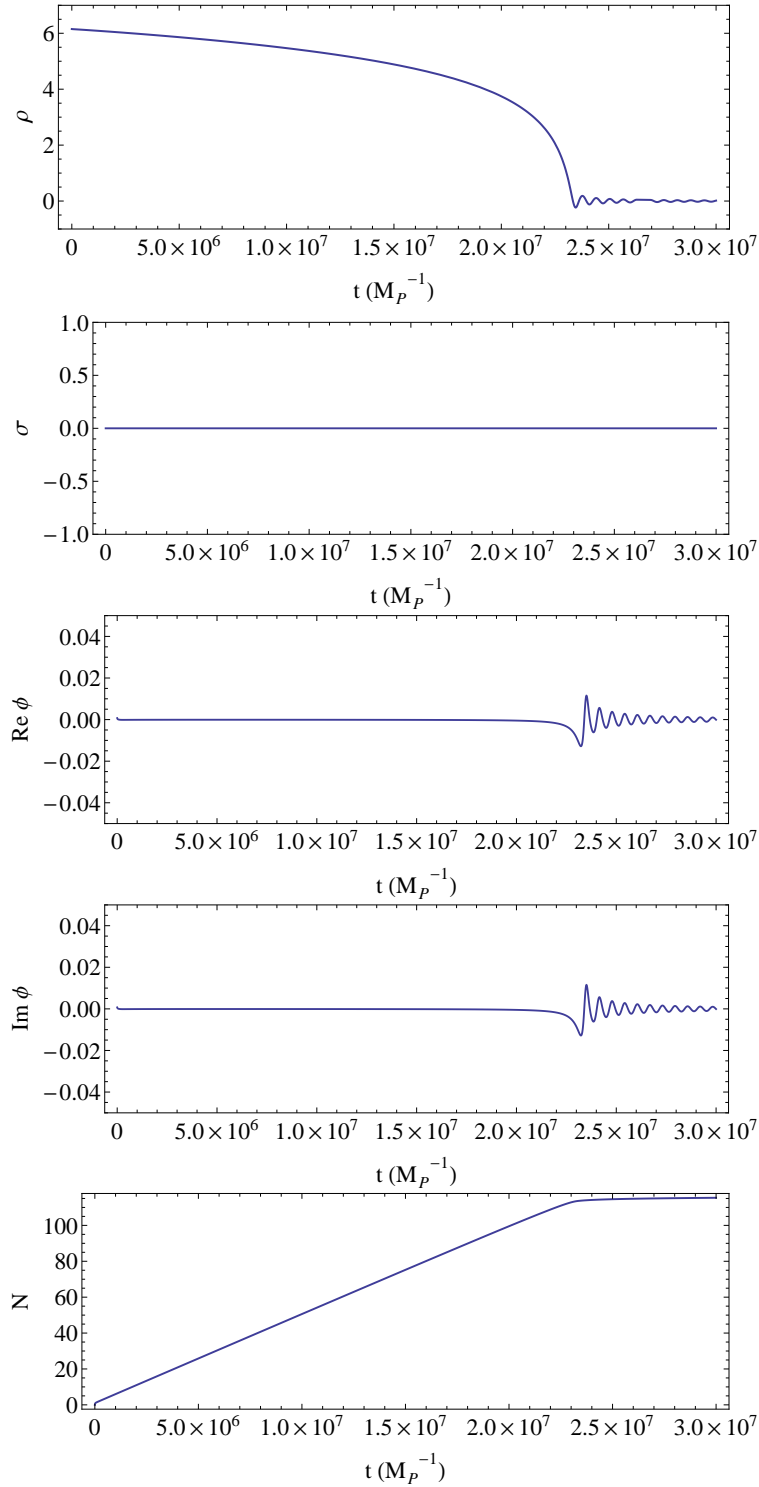


Figure 6: Numerical solution for the initial conditions $\rho_0 = 6.15$, $\sigma_0 = 0$, $\phi_0 = 0.001 + 0.001i$.

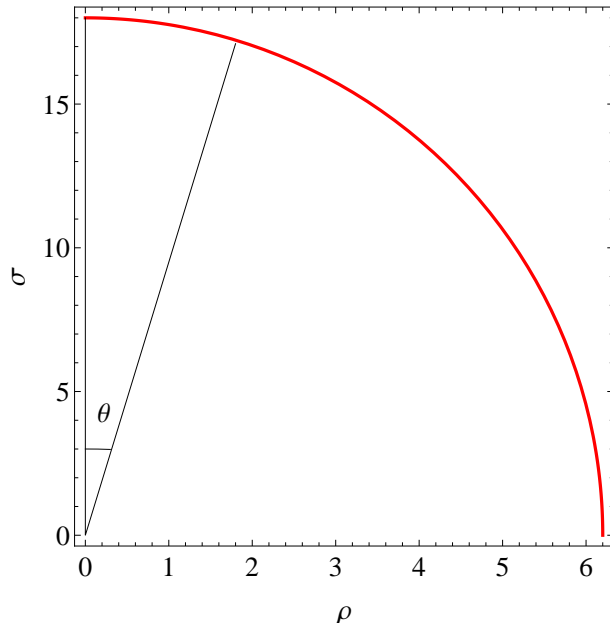


Figure 7: *Parameterization of initial conditions in the (ρ, σ) plane for $\phi_0 = 0$.*

larger field values, in which case the equivalent number e-folds effectively follow a ‘rolling start’. In this case, the inflationary observables r and n_s take different values, in general. Accordingly, we display in Fig. 10 the dependences of the scalar tilt (upper panel) and the tensor-to-scalar ratio (lower panel) on the initial value of σ [§]. As mentioned previously, the coupling between the real and imaginary parts of the complex field T perturbs the field ρ , even if it is initially stationary at its minimum $\rho = 0$. This perturbation translates into a dependence of r , in particular, on the initial value of σ , as seen in Fig. 10. The scalar tilt is almost independent of σ , plateauing when $\sigma \gtrsim 20$, whereas the tensor-to-scalar ratio decreases slowly for increasing σ , with $r \simeq 0.16$ at 50 e-foldings and $r \simeq 0.14$ at 60 e-foldings for $\sigma \gg 1$.

In the same spirit, we have explored ‘standing start’ initial conditions at arbitrary points in the (ρ, σ) plane for $\phi_0 = 0$. The results for the scalar tilt n_s are displayed using colour coding in Fig. 11 for $N = 50$ e-folds (left panel) and $N = 60$ e-folds (right panel). Here and in the two subsequent figures, the black lines mark the boundary of the region in the (ρ, σ) plane where sufficient N can be obtained. As in Figs. 8 and 9, we see that slightly lower values of n_s are possible for models intermediate between the quadratic and Starobinsky-like limits, but that always $n_s < 0.969$, within the experimental 68% CL range. The corresponding results for the tensor-to-scalar ratio r are shown in Fig. 12. As expected, we see large BICEP2-friendly values of r when $\sigma \gg \rho$, as in quadratic models of inflation, and Planck-friendly, Starobinsky-like values of r when $\rho \gg \sigma$. As already commented,

[§]The dependence on the initial value of ρ is less significant.

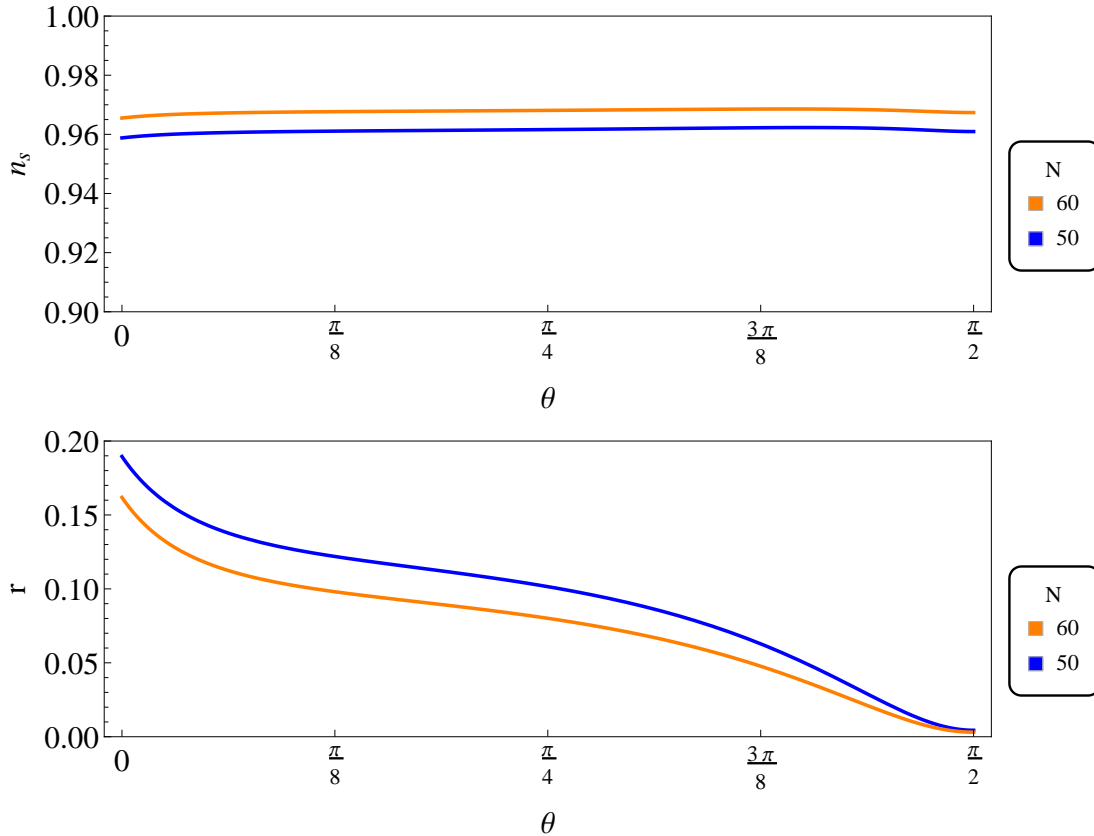


Figure 8: *Upper panel: The scalar tilt as function of θ . Lower panel: The tensor-to-scalar ratio as function of θ .*

there are large areas of parameter space where $r \sim 0.1$, which might satisfy both Planck and BICEP2.

In general, multi-field models of inflation yield enhanced amounts of non-Gaussianity. Accordingly, we have calculated the shape-independent part of the nonlinear parameter f_{NL} , denoted by $f_{NL}^{(4)}$, in the δN formalism (see, e.g., [46]). The colour-coded results for arbitrary initial conditions in the (ρ, σ) plane for $\phi_0 = 0$ are shown in Fig. 13. We see that the largest values of $f_{NL}^{(4)} \simeq 0.125$, which is far below the current experimental upper limit, and that much smaller values are found closer to the quadratic and Starobinsky-like axes, where the model resembles more closely a single-field model.

4 Supersymmetry Breaking

In the above analysis we have neglected the possible effects of supersymmetry breaking, which one would expect, in general, to have little importance for $m_{3/2} \ll m \sim 2 \times 10^{13}$ GeV.

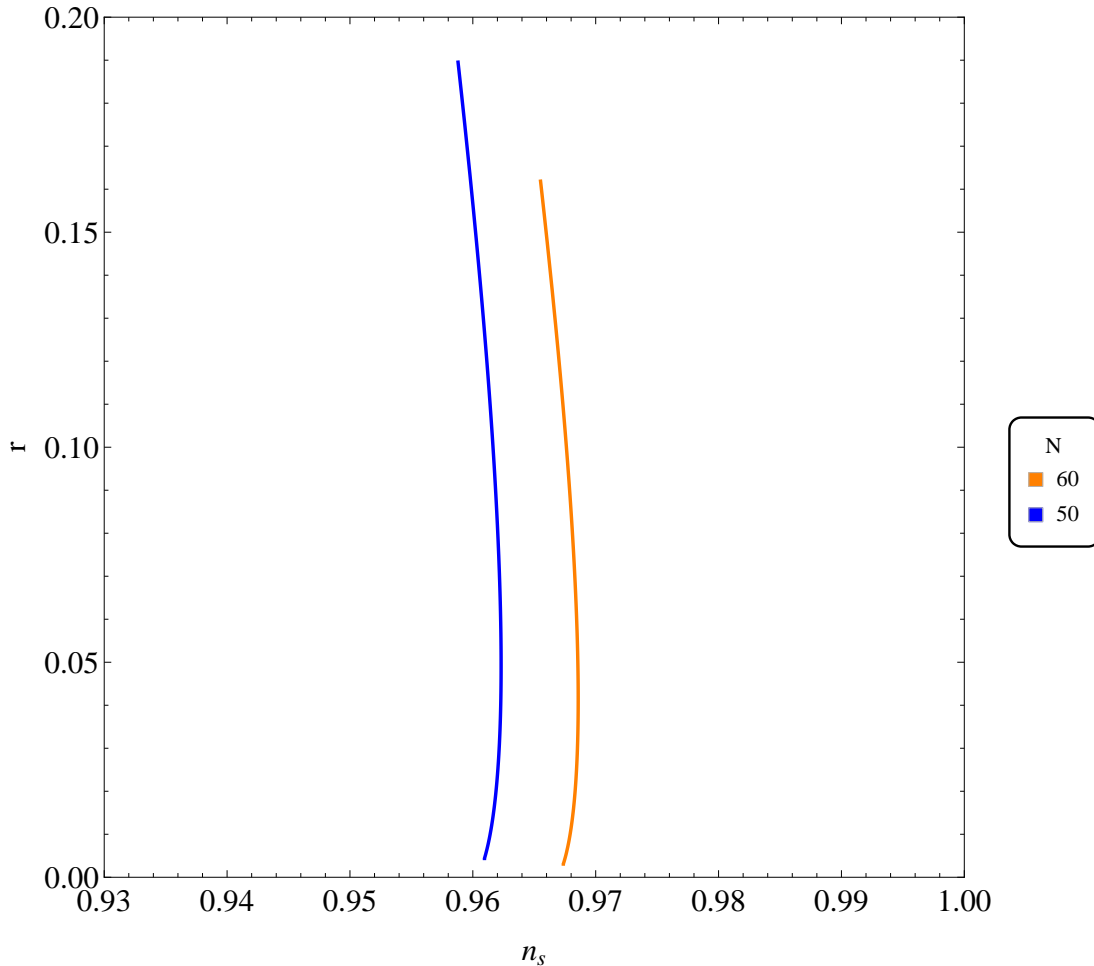


Figure 9: *The parametric curve $(n_s(\theta), r(\theta))$.*

There is certainly plenty of room between this upper limit and the lower limits imposed by Big Bang nucleosynthesis and the absence of supersymmetric particles so far at the LHC.

In principle, one could imagine that adding a constant term, W_0 , to the superpotential (5) would suffice to induce supersymmetry breaking as in [24]. However, doing so shifts the minimum from $\phi = 0, T = 1/2$, very slightly to a supersymmetry preserving AdS vacuum state [42, 50, 51] as in KKLT [52] and KL [53] models. Thus, some form of ‘uplifting’ is necessary and the restoration of a Minkowski (or slightly dS) vacuum with supersymmetry breaking is possible with simple examples of F-term uplifting [49, 54–56].

As a toy example, we consider an unstabilized Polonyi modulus [57] as the source of supersymmetry breaking. Thus, we add to our previous Kähler potential (4) the following terms

$$\Delta K = |Z|^2 + \frac{|Y|^2}{(T + \bar{T})^n}, \quad (23)$$

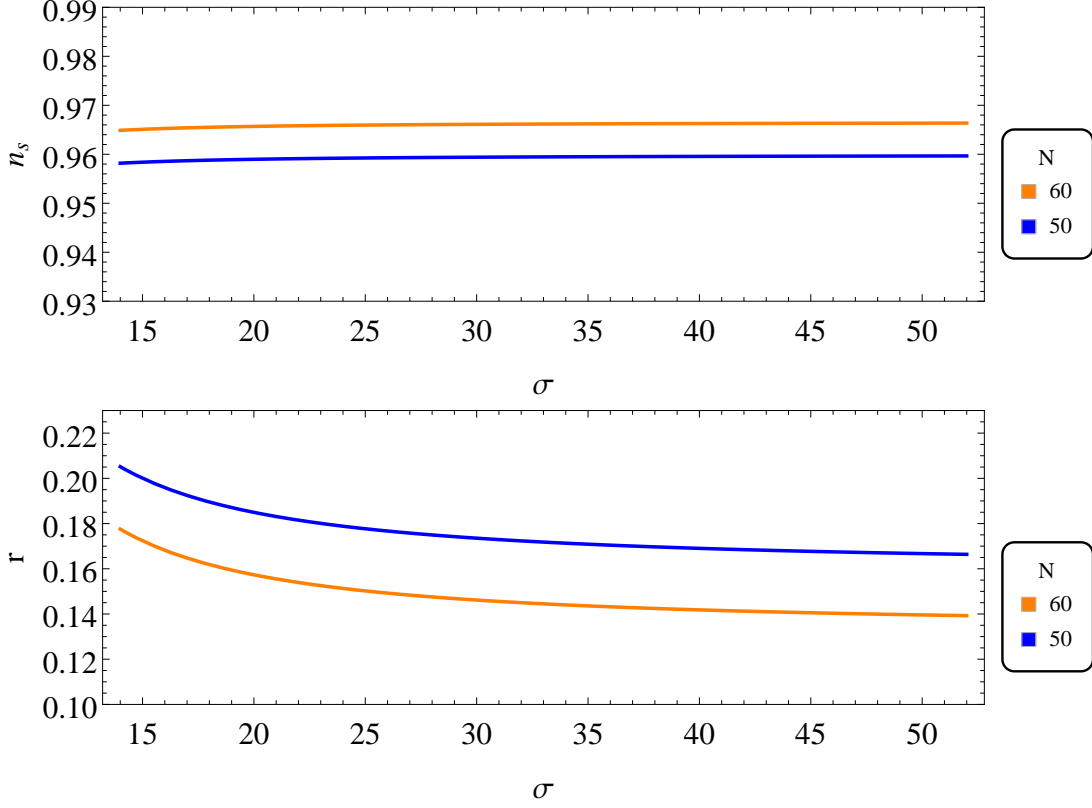


Figure 10: *Upper panel: The scalar tilt r as a function of the initial value of σ . Lower panel: The tensor-to-scalar ratio n_s as a function of the initial value of σ .*

where Z is the Polonyi field and the $\{Y\}$ are generic matter fields with unspecified modular weights. We also add to our superpotential (5) the terms

$$\Delta W = \mu(Z + \nu) + W(Y). \quad (24)$$

The scalar potential is minimized along the imaginary directions of T, ϕ and Z for

$$\text{Im } \phi = \text{Im } Z = \sigma = 0. \quad (25)$$

Along the real directions, the minimization must be performed numerically in general, since it depends on the value of μ . However, for $\mu \ll m$, the conditions

$$\partial_{\text{Re } \phi} V = \partial_{\text{Re } Z} V = \partial_{\rho} V = V = 0 \quad (26)$$

for the minimum yield, to second order in μ/m , in Planck units,

$$\text{Re } \phi \simeq \sqrt{3} \frac{\mu}{m}, \quad \rho \simeq \sqrt{6}(1 - \sqrt{3}) \left(\frac{\mu}{m}\right)^2, \quad \text{Re } Z \simeq -1 + \sqrt{3}, \quad \nu \simeq 2 - \sqrt{3}. \quad (27)$$

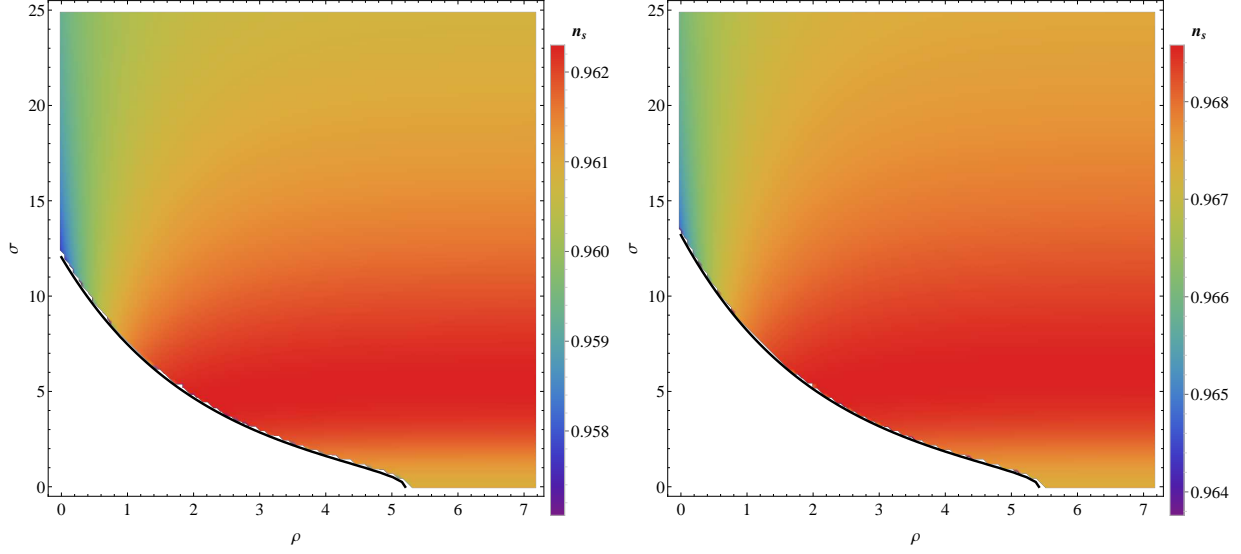


Figure 11: *The scalar tilt n_s with stationary initial conditions at arbitrary points in the (ρ, σ) plane for $\phi_0 = 0$. Left panel: The case of $N = 50$ e-foldings. Right panel: The case of $N = 60$ e-foldings. In each case, the solid curve is the boundary for the specified value of N .*

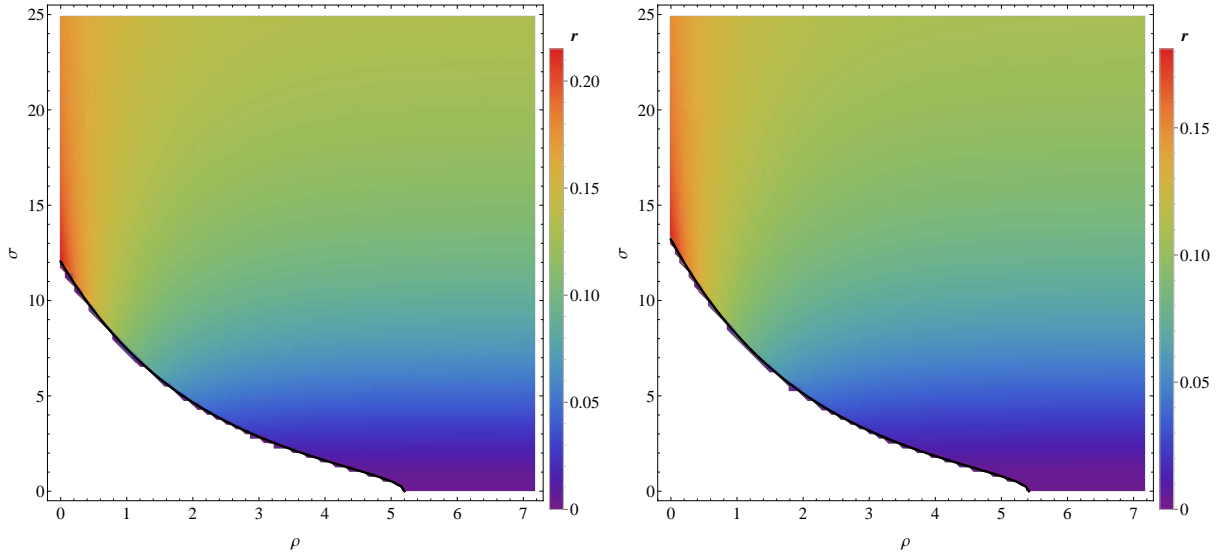


Figure 12: *The tensor-to-scalar ratio r with stationary initial conditions at arbitrary points in the (ρ, σ) plane for $\phi_0 = 0$. Left panel: The case of $N = 50$ e-foldings. Right panel: The case of $N = 60$ e-foldings. In each case, the solid curve is the boundary for the specified value of N .*

We explicitly see that the shifts in $\text{Re } \phi$ and ρ induced by the parameter μ are small when

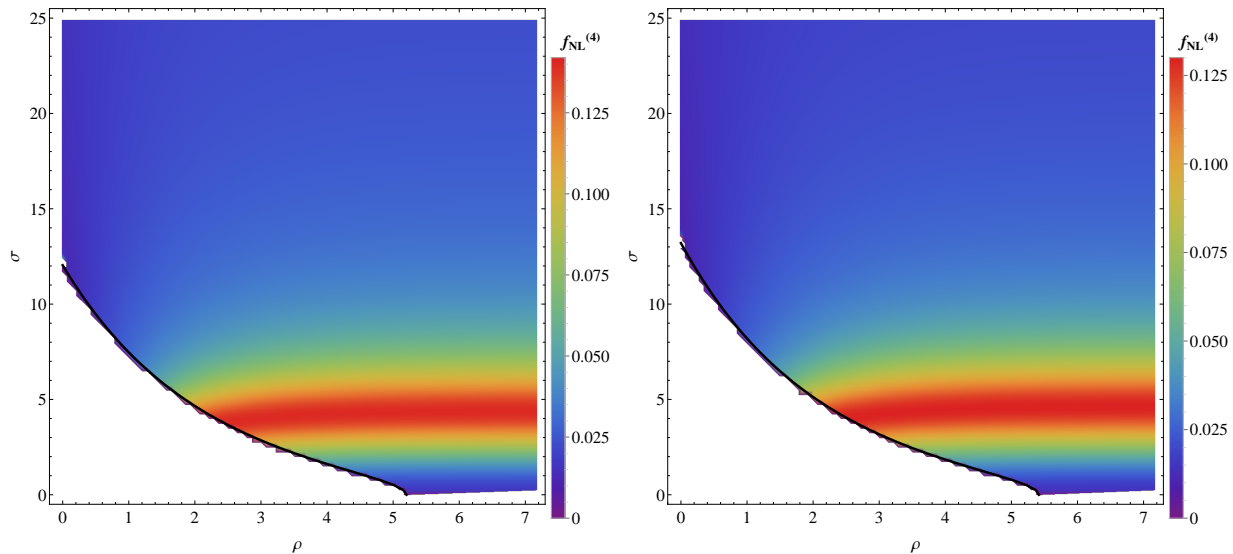


Figure 13: *The shape-independent non-Gaussianity parameter $f_{NL}^{(4)}$ with stationary initial conditions at arbitrary points in the (ρ, σ) plane for $\phi_0 = 0$. Left panel: The case of $N = 50$ e-foldings. Right panel: The case of $N = 60$ e-foldings. In each case, the solid curve is the boundary for the specified value of N .*

$\mu \ll m$. Finally, we recall that since

$$D_Z W \simeq \sqrt{3}\mu, \quad (28)$$

supersymmetry is broken with

$$m_{3/2} \simeq \mu, \quad (29)$$

and the induced masses, trilinear and bilinear terms for the matter fields $\{Y\}$ correspond to (after a constant rescaling of the superpotential $W \rightarrow e^{\sqrt{3}-2}W$)

$$m_0 \simeq m_{3/2}, \quad A_0 \simeq (3 - \sqrt{3})m_{3/2}, \quad B_0 \simeq (2 - \sqrt{3})m_{3/2}, \quad (30)$$

as in models of minimal supergravity [58]. The dependence of these parameters on the modular weight n appears at higher order in (μ/m) .

In order to avoid the well-known problems associated with the minimal Polonyi model [59], we can extend this analysis by consider stabilization [51, 56, 60] of the Polonyi field via the Kähler potential

$$\Delta K = |Z|^2 - \frac{|Z|^4}{\Lambda^2} + \frac{|Y|^2}{(T + \bar{T})^n} \quad (31)$$

with the same superpotential (24). In this case, the scalar potential is also minimized along the imaginary directions of T, ϕ and Z with $\text{Im } \phi = \text{Im } Z = \sigma = 0$.

Once again, along the real directions, the minimization must be performed numerically since it is dependent on the values of both μ and Λ . For $\Lambda \ll 1$ and $\mu \ll m$, where m is the inflaton mass, the conditions (26) can now be solved approximately to give

$$\text{Re } \phi \simeq \frac{\mu}{m}, \quad \rho \simeq -2\sqrt{\frac{2}{3}} \left(\frac{\mu}{m}\right)^2, \quad \text{Re } Z \simeq \frac{\Lambda^2}{\sqrt{12}}, \quad \nu \simeq \frac{1}{\sqrt{3}} \quad (32)$$

with higher order terms at most $\mathcal{O}(\frac{\mu}{m}\Lambda^2)$. Since

$$D_Z W \simeq \mu, \quad (33)$$

supersymmetry is broken, with

$$m_{3/2} \simeq \frac{\mu}{\sqrt{3}}, \quad (34)$$

and the induced masses, bilinear and trilinear terms for the matter fields $\{Y\}$ are

$$m_0 \simeq m_{3/2}, \quad A_0 \simeq 0, \quad B_0 \simeq -m_{3/2}, \quad (35)$$

as in minimal supergravity models with vanishing A terms or models of pure gravity mediation [61]. In this case the dependence on the modular weight n appears at $\mathcal{O}(\frac{\mu}{m}\Lambda^2)$.

5 Summary and Conclusions

We have proposed in this paper a simple two-field no-scale supergravity model of inflation whose predictions for the scalar-to-tensor perturbation ratio r interpolate between limits that are BICEP2-friendly and Planck-friendly, Starobinsky-like: $0.2 \gtrsim r \gtrsim 0.003$. As we have shown, this model also yields $n_s \sim 0.96$, as indicated by WMAP, Planck and BICEP2 data, while also yielding small values of the non-Gaussianity parameter $f_{NL}^{(4)} \lesssim 0.125$. Our model is based on the form of effective low-energy field theory derived from orbifold compactifications of string theory, and can accommodate a Polonyi mechanism for supersymmetry breaking that is suitable for particle phenomenology.

We await with interest confirmation of the B-mode polarization measurement made by BICEP2, and verification that is mainly of primordial origin. In the mean time, we note that over large regions of its parameter space our no-scale model yields $r \sim 0.1$, which may be compatible at the 68% CL with each of the WMAP, Planck and BICEP2 measurements. In that sense, our model may indeed ‘fit them all’.

Acknowledgements

The work of J.E. was supported in part by the London Centre for Terauniverse Studies (LCTS), using funding from the European Research Council via the Advanced Investigator Grant 267352 and from the UK STFC via the research grant ST/J002798/1. J.E. also thanks Hong-Jian He for his kind hospitality at the Center for High Energy Physics, Tsinghua University, and S.-H. Henry Tye for his kind hospitality at the Institute for Advanced Study, Hong Kong University of Science and Technology, while this work was being carried out. The work of D.V.N. was supported in part by the DOE grant DE-FG03-95-ER-40917 and would like to thank A.P. for inspiration. The work of M.A.G.G. and K.A.O. was supported in part by DOE grant DE-FG02-94-ER-40823 at the University of Minnesota.

References

- [1] P. A. R. Ade *et al.* [Planck Collaboration], arXiv:1303.5082 [astro-ph.CO].
- [2] G. Hinshaw *et al.* [WMAP Collaboration], *Astrophys. J. Suppl.* **208** (2013) 19 [arXiv:1212.5226 [astro-ph.CO]]; for a recent review, see E. Komatsu *et al.* [on behalf of the WMAP Science Team Collaboration], arXiv:1404.5415 [astro-ph.CO].
- [3] K. A. Olive, *Phys. Rept.* **190** (1990) 307; A. D. Linde, *Particle Physics and Inflationary Cosmology* (Harwood, Chur, Switzerland, 1990); D. H. Lyth and A. Riotto, *Phys. Rep.* **314** (1999) 1 [arXiv:hep-ph/9807278]; For a recent encyclopedic review see: J. Martin, C. Ringeval and V. Vennin, arXiv:1303.3787 [astro-ph.CO] and references therein.
- [4] P. A. R. Ade *et al.* [BICEP2 Collaboration], arXiv:1403.3985 [astro-ph.CO].
- [5] K. M. Smith, C. Dvorkin, L. Boyle, N. Turok, M. Halpern, G. Hinshaw and B. Gold, arXiv:1404.0373 [astro-ph.CO].
- [6] C. R. Contaldi, M. Peloso and L. Sorbo, arXiv:1403.4596 [astro-ph.CO]; V. Miranda, W. Hu and P. Adshead, arXiv:1403.5231 [astro-ph.CO].
- [7] H. Liu, P. Mertsch and S. Sarkar, arXiv:1404.1899 [astro-ph.CO].
- [8] A. D. Linde, *Nucl. Phys. B* **252**, 153 (1985); M. S. Madsen and P. Coles, *Nucl. Phys. B* **298**, 701 (1988).
- [9] A. A. Starobinsky, *Phys. Lett. B* **91**, 99 (1980).

- [10] V. F. Mukhanov and G. V. Chibisov, JETP Lett. **33**, 532 (1981) [Pisma Zh. Eksp. Teor. Fiz. **33**, 549 (1981)].
- [11] A. A. Starobinsky, Sov. Astron. Lett. **9**, 302 (1983).
- [12] J. R. Ellis, D. V. Nanopoulos, K. A. Olive and K. Tamvakis, Phys. Lett. B **118** (1982) 335; Phys. Lett. B **120** (1983) 331; Nucl. Phys. B **221** (1983) 52.
- [13] D. V. Nanopoulos, K. A. Olive, M. Srednicki and K. Tamvakis, Phys. Lett. B **123**, 41 (1983).
- [14] R. Holman, P. Ramond and G. G. Ross, Phys. Lett. B **137**, 343 (1984).
- [15] J. R. Ellis, K. Enqvist, D. V. Nanopoulos, K. A. Olive and M. Srednicki, Phys. Lett. B **152** (1985) 175 [Erratum-ibid. **156B** (1985) 452].
- [16] A. B. Goncharov and A. D. Linde, Phys. Lett. B **139**, 27 (1984).
- [17] D. Z. Freedman, P. van Nieuwenhuizen and S. Ferrara, Phys. Rev. D **13** (1976) 3214; S. Deser and B. Zumino, Phys. Lett. B **62** (1976) 335.
- [18] E. J. Copeland, A. R. Liddle, D. H. Lyth, E. D. Stewart and D. Wands, Phys. Rev. D **49**, 6410 (1994) [astro-ph/9401011]; E. D. Stewart, Phys. Rev. D **51**, 6847 (1995) [hep-ph/9405389].
- [19] E. Cremmer, S. Ferrara, C. Kounnas and D. V. Nanopoulos, Phys. Lett. B **133** (1983) 61; J. R. Ellis, A. B. Lahanas, D. V. Nanopoulos and K. Tamvakis, Phys. Lett. B **134** (1984) 429.
- [20] A. B. Lahanas and D. V. Nanopoulos, Phys. Rept. **145** (1987) 1.
- [21] E. Witten, Phys. Lett. B **155** (1985) 151.
- [22] J. Ellis, D. V. Nanopoulos and K. A. Olive, Phys. Rev. Lett. **111** (2013) 111301 [arXiv:1305.1247 [hep-th]];
- [23] J. Ellis, D. V. Nanopoulos and K. A. Olive, JCAP **1310** (2013) 009 [arXiv:1307.3537 [hep-th]];
- [24] J. Ellis, D. V. Nanopoulos and K. A. Olive, Phys. Rev. D **89**, 043502 (2014) [arXiv:1310.4770 [hep-ph]].
- [25] J. Alexandre, N. Houston and N. E. Mavromatos, Phys. Rev. D **89** (2014) 027703 [arXiv:1312.5197 [gr-qc]]; J. Ellis, N. E. Mavromatos and D. V. Nanopoulos, arXiv:1402.5075 [hep-th].

- [26] J. Ellis, M. A. G. García, D. V. Nanopoulos and K. A. Olive, arXiv:1403.7518 [hep-ph].
- [27] R. Kallosh and A. Linde, JCAP **1306**, 028 (2013) [arXiv:1306.3214 [hep-th]].
- [28] W. Buchmuller, V. Domcke and K. Kamada, Phys. Lett. B **726**, 467 (2013) [arXiv:1306.3471 [hep-th]].
- [29] F. Farakos, A. Kehagias and A. Riotto, Nucl. Phys. B **876**, 187 (2013) [arXiv:1307.1137].
- [30] S. Ferrara, R. Kallosh, A. Linde and M. Porrati, Phys. Rev. D **88**, no. 8, 085038 (2013) [arXiv:1307.7696 [hep-th]]; S. Ferrara, R. Kallosh, A. Linde and M. Porrati, JCAP **1311**, 046 (2013) [arXiv:1309.1085 [hep-th], arXiv:1309.1085]; S. Ferrara, R. Kallosh and A. Van Proeyen, JHEP **1311**, 134 (2013) [arXiv:1309.4052 [hep-th]]; S. Cecotti and R. Kallosh, arXiv:1403.2932 [hep-th].
- [31] C. Pallis, arXiv:1312.3623 [hep-ph].
- [32] S. Ferrara, A. Kehagias and A. Riotto, arXiv:1403.5531 [hep-th].
- [33] R. Kallosh, A. Linde, B. Vercnocke and W. Chemissany, arXiv:1403.7198 [hep-th]; K. Hamaguchi, T. Moroi and T. Terada, arXiv:1403.7521 [hep-ph].
- [34] S. Cecotti, Phys. Lett. B **190** (1987) 86.
- [35] A. S. Goncharov and A. D. Linde, Class. Quant. Grav. **1**, L75 (1984).
- [36] P. Binétruy and M. K. Gaillard, Phys. Rev. D **34**, 3069 (1986).
- [37] H. Murayama, H. Suzuki, T. Yanagida and J. Yokoyama, Phys. Rev. D **50**, 2356 (1994) [arXiv:hep-ph/9311326].
- [38] S. C. Davis and M. Postma, JCAP **0803**, 015 (2008) [arXiv:0801.4696 [hep-ph]].
- [39] S. Antusch, M. Bastero-Gil, K. Dutta, S. F. King and P. M. Kostka, JCAP **0901**, 040 (2009) [arXiv:0808.2425 [hep-ph]].
- [40] S. Antusch, M. Bastero-Gil, K. Dutta, S. F. King and P. M. Kostka, Phys. Lett. B **679**, 428 (2009) [arXiv:0905.0905 [hep-th]].
- [41] R. Kallosh and A. Linde, JCAP **1011**, 011 (2010) [arXiv:1008.3375 [hep-th]]; R. Kallosh, A. Linde and T. Rube, Phys. Rev. D **83**, 043507 (2011) [arXiv:1011.5945 [hep-th]].

- [42] R. Kallosh, A. Linde, K. A. Olive and T. Rube, Phys. Rev. D **84**, 083519 (2011) [arXiv:1106.6025 [hep-th]].
- [43] W. Buchmuller, C. Wieck and M. W. Winkler, arXiv:1404.2275 [hep-th].
- [44] L. J. Dixon, V. Kaplunovsky and J. Louis, Nucl. Phys. B **329** (1990) 27.
- [45] J. A. Casas, in *Proceedings, International Europhysics Conference on High-Energy Physics*, Jerusalem, Israel, August 19-25, 1997, eds. D. Lellouch, G. Mikenberg and E. Rabinovici, pp 914-917 [hep-ph/9802210].
- [46] F. Vernizzi and D. Wands, JCAP **0605** (2006) 019 [astro-ph/0603799].
- [47] D. Croon, J. Ellis and N. E. Mavromatos, Physics Letters B **724** (2013) , 165 [arXiv:1303.6253 [astro-ph.CO]].
- [48] J. Ellis, N. E. Mavromatos and D. J. Mulryne, arXiv:1401.6078 [astro-ph.CO].
- [49] O. Lebedev, H. P. Nilles and M. Ratz, Phys. Lett. B **636**, 126 (2006) [hep-th/0603047].
- [50] A. Linde, Y. Mambrini and K. A. Olive, Phys. Rev. D **85** (2012) 066005 [arXiv:1111.1465 [hep-th]].
- [51] E. Dudas, A. Linde, Y. Mambrini, A. Mustafayev and K. A. Olive, Eur. Phys. J. C **73** (2013) 2268 [arXiv:1209.0499 [hep-ph]].
- [52] S. Kachru, R. Kallosh, A. D. Linde and S. P. Trivedi, Phys. Rev. D **68**, 046005 (2003) [arXiv:hep-th/0301240].
- [53] R. Kallosh and A. D. Linde, JHEP **0412**, 004 (2004) [arXiv:hep-th/0411011]; J. J. Blanco-Pillado, R. Kallosh and A. D. Linde, JHEP **0605**, 053 (2006) [hep-th/0511042]; R. Kallosh and A. D. Linde, JCAP **0704**, 017 (2007) [arXiv:0704.0647 [hep-th]].
- [54] M. Gomez-Reino and C. A. Scrucca, JHEP **0605**, 015 (2006) [hep-th/0602246].
- [55] E. Dudas, C. Papineau and S. Pokorski, JHEP **0702**, 028 (2007) [hep-th/0610297]; H. Abe, T. Higaki, T. Kobayashi and Y. Omura, Phys. Rev. D **75**, 025019 (2007) [hep-th/0611024]; H. Abe, T. Higaki and T. Kobayashi, Phys. Rev. D **76**, 105003 (2007) [arXiv:0707.2671 [hep-th]].
- [56] R. Kallosh and A. D. Linde, JHEP **0702**, 002 (2007) [hep-th/0611183].
- [57] J. Polonyi, Budapest preprint KFKI-1977-93 (1977).

- [58] R. Barbieri, S. Ferrara and C. A. Savoy, *Phys. Lett. B* **119**, 343 (1982).
- [59] G. D. Coughlan, W. Fischler, E. W. Kolb, S. Raby and G. G. Ross, *Phys. Lett. B* **131**, 59 (1983); A. S. Goncharov, A. D. Linde, M. I. Vysotsky, *Phys. Lett.* **B147**, 279 (1984); J. Ellis, D. V. Nanopoulos, and M. Quiros, *Phys. Lett. B* **174**, 176 (1986); T. Banks, D. B. Kaplan and A. E. Nelson, *Phys. Rev. D* **49**, 779 (1994) [hep-ph/9308292]; B. De Carlos, J. A. Casas, F. Quevedo, E. Roulet, *Phys. Lett. B* **318**, 447 (1993) [hep-ph/9308325].
- [60] M. Dine, R. Kitano, A. Morisse and Y. Shirman, *Phys. Rev. D* **73**, 123518 (2006) [hep-ph/0604140]; R. Kitano, *Phys. Lett. B* **641**, 203 (2006) [hep-ph/0607090]; J. Fan, M. Reece and L.-T. Wang, *JHEP* **1109**, 126 (2011) [arXiv:1106.6044 [hep-ph]]; K. Harigaya, M. Ibe, K. Schmitz and T. T. Yanagida, *Phys. Lett. B* **721**, 86 (2013) [arXiv:1301.3685 [hep-ph]]; M. Bose, M. Dine and P. Draper, *Phys. Rev. D* **88**, 023533 (2013) [arXiv:1305.1066 [hep-ph]]; M. A. G. Garcia and K. A. Olive, *JCAP* **1309**, 007 (2013) [arXiv:1306.6119 [hep-ph]]; J. L. Evans, M. A. G. Garcia and K. A. Olive, *JCAP* **1403**, 022 (2014) [arXiv:1311.0052 [hep-ph]].
- [61] J. L. Evans, M. Ibe, K. A. Olive and T. T. Yanagida, *Eur. Phys. J. C* **73**, 2468 (2013) [arXiv:1302.5346 [hep-ph]]; J. L. Evans, K. A. Olive, M. Ibe and T. T. Yanagida, *Eur. Phys. J. C* **73**, 2611 (2013) [arXiv:1305.7461 [hep-ph]].